Particle Size Effects on the Strength and Fabric of Granular Media

Kevin C. Kuei, S.M.ASCE¹; Jason T. DeJong, M.ASCE²; and Alejandro Martinez, M.ASCE³

ABSTRACT

The reliance on sand-based methods for the characterization and design of gravelly soils is necessitated in part by a limited understanding of how to account for the effects of particle size and distribution. In this paper, particle size effects on the strength and fabric of cohesionless, granular media are investigated using the discrete element method by testing specimens with particle size distributions (PSDs) of differing coefficient of uniformity (C_U) and mean grain size (d_{50}). Preliminary results show that when all particle shape characteristics are equal, increasing d_{50} yields equivalent stress-strain responses for the same relative density (D_R) and C_U . However, when increasing C_U , specimens exhibit more dilative tendencies and greater shear strengths. Increasing C_U results in more dispersive distributions of contact force, stress, and coordination number. The void ratios associated with minimum and maximum density, and constant volume conditions during shear also decrease with increasing C_U .

MOTIVATION

The characterization, and design of structures composed of or interacting with gravelly soils is challenging in geotechnical practice. Sand-based methods are routinely assumed to be applicable for gravelly deposits. This assumption is necessitated in part due to limited case histories and understanding of how to account for particle size effects, or for lack of better alternatives. Moreover, inconsistent, or even conflicting interpretations between past studies on particle size effects due to inadequate experimental control may contribute to the ambiguity in the current state of practice. As Sturm et al. (2019) notes, widely graded gravelly soils can exhibit a wide range of attributes beyond particle size that influence their properties and behavior. Thus, the study of gravelly soils and how their behavior may differ from sand-based counterparts requires careful and systematic examination, and a consistent framework for evaluation (e.g. same depositional environment, or explicit accounting for particle shape effects). A particle size study combining materials from different depositional environments for example, may be suitable for engineered structures, but not representative of naturally encountered deposits; in addition, compensating particle size and particle shape effects may produce ambiguous or unrepresentative results to those encountered in the field.

More recent experimental and numerical studies both acknowledging and satisfying these more rigorous constraints (e.g. Sturm et al., 2019; Yang and Luo, 2017; Liu et al, 2014) have begun to emerge, but there is still limited understanding in this area. This paper presents initial results of numerical simulations with the discrete element method on specimens of differing polydispersity in order to develop additional insight of how particle size effects influence the strength, fabric, and behavior of coarse-grained media (e.g. sands, gravels), while controlling for

¹Dept. of Civil and Environmental Engineering, Univ. of California at Davis, Davis, CA. E-mail: kckuei@ucdavis.edu

²Dept. of Civil and Environmental Engineering, Univ. of California at Davis, Davis, CA. E-mail: jdejong@ucdavis.edu

³Dept. of Civil and Environmental Engineering, Univ. of California at Davis, Davis, CA. E-mail: amart@ucdavis.edu

particle shape effects.

METHODS AND NUMERICAL TOOLS

Particle Size Distributions: To investigate the particle size effects, tests were conducted on specimens composed of spherical particles sampled from log-linear cumulative distribution functions with different mean grain size (d_{50}) and coefficient of uniformity (C_U). Log-linear distributions were used for their simplicity, and based on initial sensitivity tests which indicated that slightly skewed tails had only a minor effect on the mechanical response. In total, seven particle size distributions with d_{50} ranging from 2.4 to 29.4 mm and C_U ranging from 1.0 to 3.9 were considered. Figure 1 illustrates the different particle size distributions tested, ranging from a coarse sand to a coarse gravel, including their mixtures.

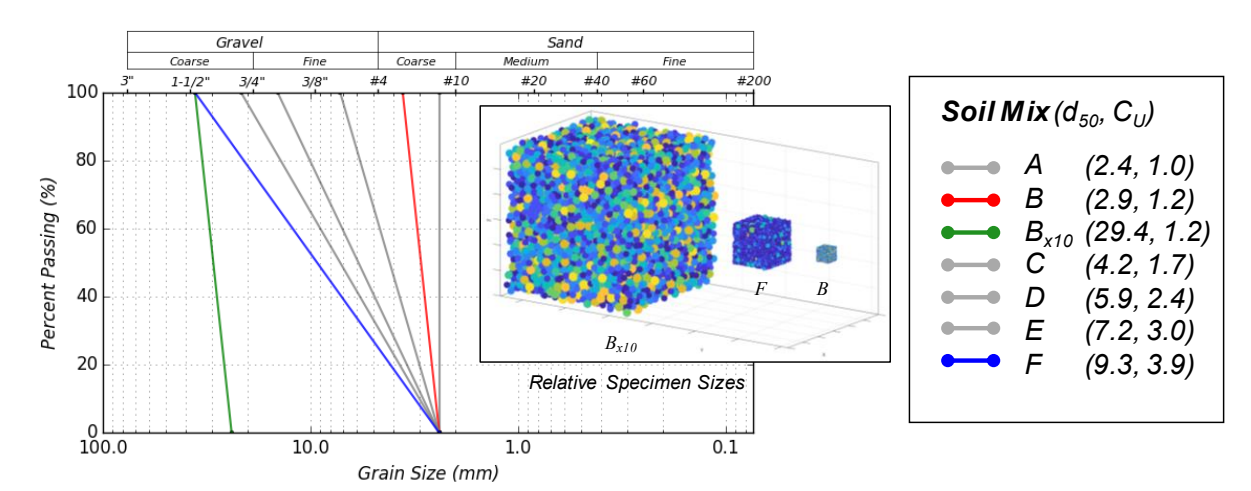


Figure 1. Particle size distributions and relative specimen sizes used in simulations.

The design of the distributions were motivated to probe two questions: the effect of mean grain size (d_{50}) when the shape of the gradation (i.e., C_U) is held constant—in other words, how does a coarse sand compare with a coarse gravel when particle size effects are isolated (e.g. Mix B and Mix B_{x10}); as well as the effect of systematically widening the gradation (or increasing C_U) from a clean sand, where most geotechnical engineering correlations are centered, towards a more gravelly particle size composition (e.g. Mix A to Mix F).

DEM Model, Simulation, and Preparation Procedures: Three-dimensional numerical simulations of isotopically consolidated drained (ICD) triaxial compression (TXC) tests were performed using the commercial discrete-element code, Itasca PFC3D (for Particle Flow Code in Three Dimensions) version 5.00.33. The basic model configuration and components are illustrated in Figure 2a. Cubical representative volume elements (RVE's) with periodic vertical and horizontal boundaries form the basis of all simulations in this study. Periodic boundary conditions were selected to eliminate boundary effects associated with stiff walls, avoid localization (shear banding), and encourage more homogenous deformation fields (Huang et al, 2014; Cundall, 1988; Hanley et al., 2015). Inspection of specimen sections of particle spin and velocity during simulations generally corroborated the absence of localization effects. A measurement sphere is situated at the center of specimens for stress monitoring, and accumulating changes in strain and void ratio. Drained, or equivalent undrained conditions can be achieved trivially through assignment of strain-, or stress-based servo-controlled boundaries to maintain strict volumetric control, or maintain principal stresses in a given direction,

respectively. Stress-based servo-controlled algorithms similar to those described in Thornton (2000) are employed at the horizontal boundaries in this study.

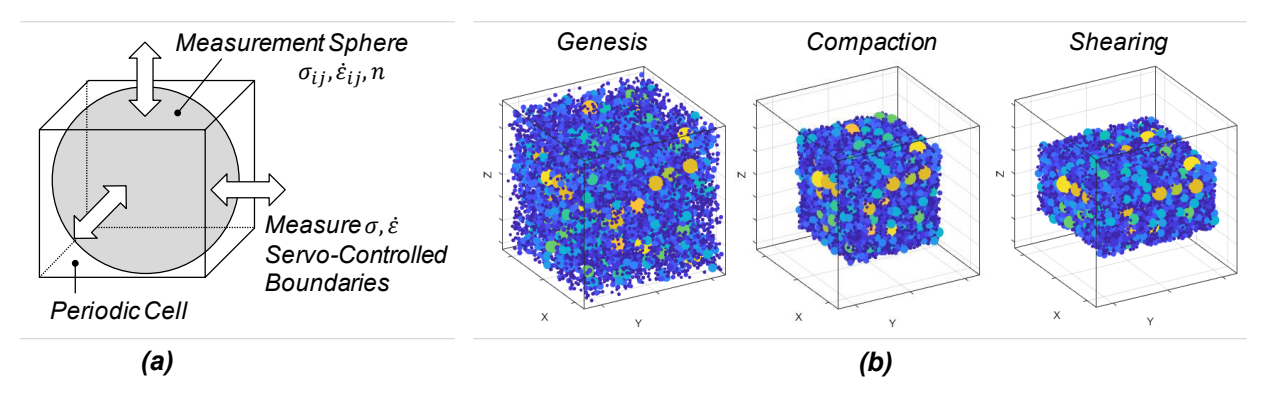


Figure 2. DEM modelling: (a) triaxial model, and (b) simulation stages.

The different simulation stages involved from specimen preparation to shearing are illustrated in Figure 2b. In the first stage of specimen genesis, particles are generated with initial temporary friction assignments, and a high initial porosity. Due to the generation algorithm, particles can have large initial overlaps. Consequently, a relaxation stage is applied until overlap ratios become small and a near-zero mean stress state is achieved. Following relaxation, the specimen is compacted using a domain distortion technique (e.g. Gonzales, 2009; Imole et al., 2013) which applies an isotropic strain field to the entire specimen until a target stress state is attained. This creates a near-isotropic fabric within the specimens. At the end of compaction and just before shearing, final particle friction coefficients are assigned. During the shearing stage, vertical boundaries are displaced at a constant axial strain rate, while horizontal boundaries self-adjust to maintain the initial confining stress during shear. It is noted that domain distortion is used during compaction to achieve more homogenous specimens, whereas boundary contraction rather than domain distortion is used during the shearing stage to better reflect the loading conditions of physical experiments (e.g. Zhang and Evans, 2018).

The minimum and maximum void ratios (e_{min} and e_{max}) are void ratio indices commonly measured in the laboratory for the purpose of calculating relative density (D_R). In this study, e_{min} and e_{max} are defined conveniently as the densest and loosest states, respectively, corresponding to compaction with zero and full interparticle friction at a given consolidation stress (p'_c) to enable D_R comparisons. Specimens of intermediate density can be achieved by allowing the initial interparticle friction coefficients to range between zero and their full value before shear (μ_c , μ_c , r_r). For each of the particle size distributions shown in Figure 1, five-point compaction curves were generated to map the (μ_c , μ_c , r_r) values required to achieve a given target void ratio (or D_R). It is noted that the approach adopted here is similar, though not identical to the one used by Wood and Maeda (2008).

A linear contact model is adopted for this study which is routinely used for DEM studies. Both a sliding and rolling resistance frictional component is used to better reflect the kinematics encountered at the particle scale. A limitation of the linear model is that particle stiffness is somewhat arbitrary, whereas with a Hertzian model, particle stiffness varies as a function of particle size—a necessary prerequisite for studies on particle size effects (Yan and Dong, 2011). Accordingly, in this study, stiffness assignments are made based on a constant normal stiffness to particle radius ratio (kn/r) which approximates Hertzian behavior. Table 1 summarizes the key model assumptions and parameters. Although no specific calibration was performed, it is noted

that the frictional values correspond roughly to a sub-rounded Ottawa sand.

Table 1. DEM Simulation Parameters, Model Assumptions

Input Parameter	Symbol	Value
Normal Stiffness to Particle Radius Ratio (N/m²)	k_n/r	$1x10^{8}$
Normal to Shear Stiffness Ratio	k_n/k_s	1.5
Sliding Friction	μ	0.4
Rolling Friction	μ_{rr}	0.175
Particle Density (kg/m³)	$ ho_{\scriptscriptstyle S}$	2,650
Local Damping	β	0.6

The total number of particles used in simulations ranged from approximately 10,000 to 50,000 for mono-size assemblages to the most widely graded assemblages, resulting in the relative specimen sizes shown in Figure 1. Hill (1956) suggests that that minimum RVE dimension to mean particle size ratio (d_{RVE}/d_{50}) should generally be greater than 1,000 to avoid the influence of microscopic heterogeneities. However, in practice, most studies must accommodate much lower ratios due to pragmatic restrictions (O'Sullivan, 2011). A review of other DEM studies investigating particle size effects indicates that $d_{RVE}/d_{50} \ge 10$ is generally consistent with the existing body of literature. In this study, d_{RVE}/d_{50} ranges from 12 to 20. Specimens were prepared to a D_R of 100% and p'_c of 100 kPa for all tests. Gravity was not considered. In all simulations, inertia numbers were less than 2.5e-3, indicating that pseudo-static conditions were maintained (da Cruz et al., 2005).

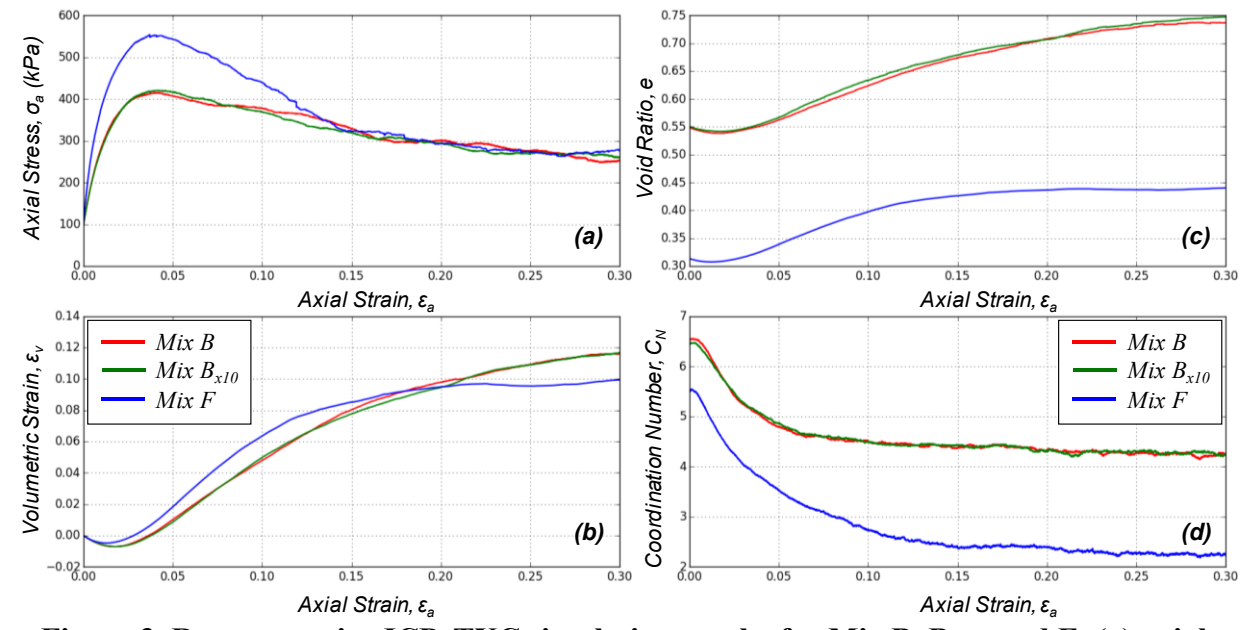


Figure 3. Representative ICD-TXC simulation results for Mix B, B_{x10} , and F: (a) axial stress, (b) volumetric strain, (c) void ratio, and (d) coordination number versus axial strain.

RESULTS AND DISCUSSION

Effect of Gradation on Mechanical Behavior: Figure 3 presents representative results from TXC simulations on three PSD's prepared to the same D_R (Mix B, Mix B_{x10}, and Mix F). Figure

3a to 3d shows the axial stress, volumetric strain, void ratio, and mean coordination number versus axial strain, respectively. It is evident from Figure 3 that changing d_{50} (i.e. Mix B and Mix B_{x10}) has a negligible effect on the mechanical response when D_R and C_U are held constant. In other words, a coarse-grained sand behaves as a coarse-grained gravel when particle shape effects are isolated. However, it is observed that Mix F mobilizes a higher peak shear strength than Mix B and Mix B_{x10} . Inspection of other spaces also indicates that Mix F develops a higher dilatancy angle, and dilates from a smaller initial void ratio for the same D_R .

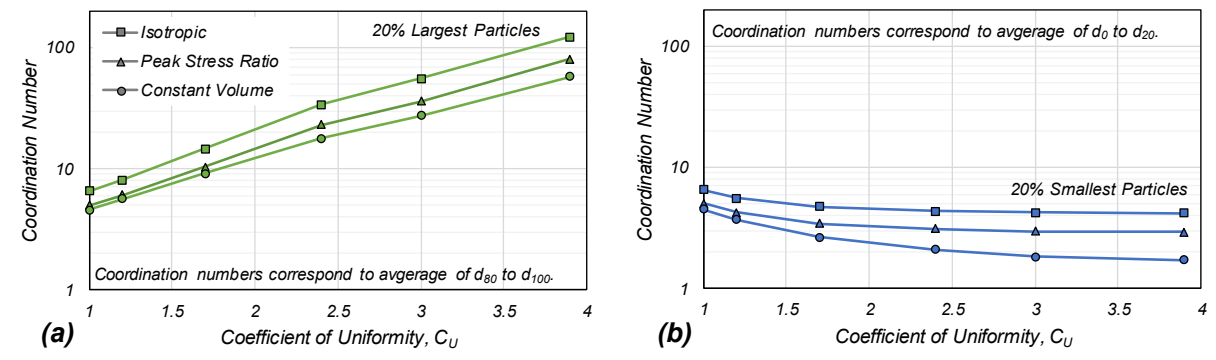


Figure 4. Coordination numbers for (a) largest, and (b) smallest, 20% of particles by mass.

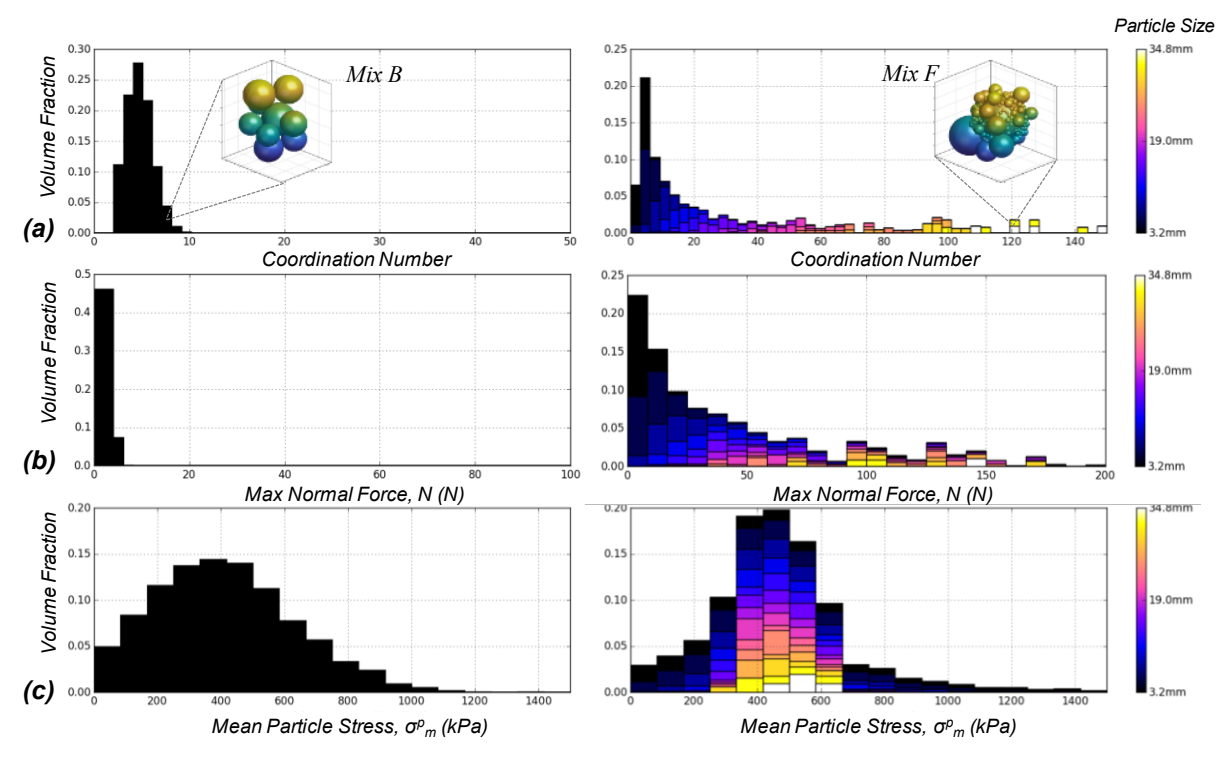


Figure 5. Comparison of fabric quantities for Mix B and Mix F at peak stress ratio: (a) coordination number, (b) max normal force, and (c) mean particle stress.

Perhaps counterintuitively, the mean coordination number (C_N) decreases when the gradation becomes wider. Inspection of mean coordination number by particle mass fraction ranges (i.e. volumetric coordination numbers) suggest that the low values are due to an averaging effect, and that this is a limitation of the traditional mean, or "mechanical" coordination number

counterparts when dealing with widely graded soils. Figure 4a and 4b shows the volumetric coordination values for the smallest, and largest 20% of particles by mass, respectively, for all mixes at end of compaction, at peak stress ratio, and constant volume conditions. The results indicate very large coordination values for the largest particles, and coordination values for the smallest particles which align more closely with the global average.

Effect of Gradation on Fabric: Figure 5 presents a more detailed comparison of microstructural changes in select fabric quantities when moving from mono-size to more widely graded assemblages. Figure 5a to 5b shows the mass fraction distributions for coordination number, maximum contact force, and mean particle stress, respectively for Mix B and Mix F (neglecting floaters or rattlers). The contribution of a given particle size bin is also indicated by the variation in colors. Thus, Mix F, being widely graded, shows several particle sizes whereas the solid color of Mix B indicates a relatively uniform specimen.

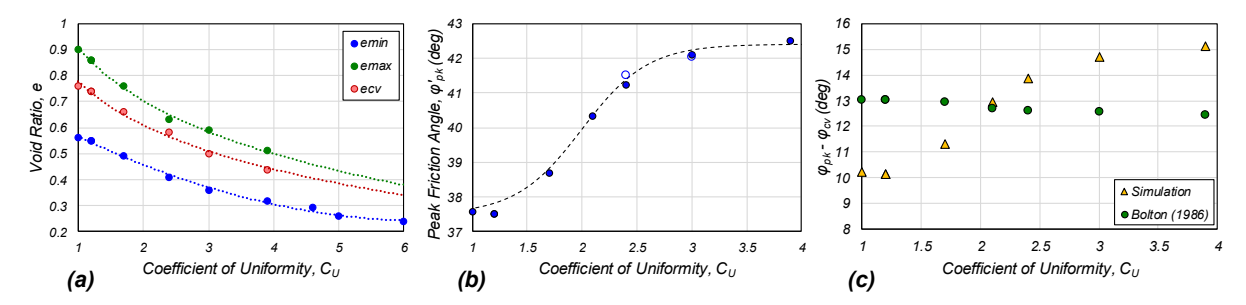


Figure 6. Effect of coefficient of uniformity on (a) void ratio indices, (b) peak friction angle, and (c) stress-dilatancy behavior.

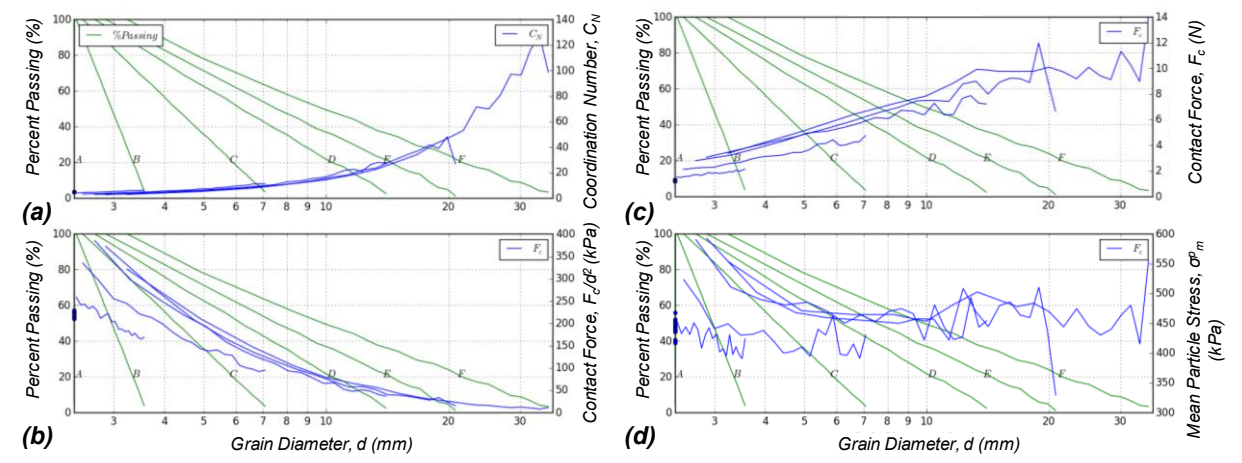


Figure 7. Effect of C_U on fabric quantities at peak stress ratio: (a) coordination number, (b) normalized contact force, (c) contact force, and (d) mean particle stress by grain size bin.

The trends clearly indicate that distributions become increasingly disperse as C_U increases. Moreover, a natural grading, or separation between the largest, smallest, and neighboring particles arises, with the largest particles generally having the highest coordination values, and carrying the highest contact forces, and the smallest particles have the lowest coordination values, and sustaining the lowest contact forces. These observations on coordination appear consistent with literature; Wood and Maeda (2008) qualitatively make this connection, while Yi et al. (2011) demonstrate using ternary mixtures that the number of large-to-small contacts increases, and small-to-small contacts decreases with increasing polydispersity.

The trend is somewhat different when considering mean particle stresses, as particle stresses factor in both the magnitude of contact forces, as well as the geometry of surrounding contacts, and suggest that the largest particles tend to congregate near the center of the distribution. In contrast, the smallest particles span the tails and can have either very high, or relatively low stresses. Although not considered in the present simulations, these findings are relevant to problems related to particle crushing and probability of survival, which generally suggest that the smallest particles tend to be most susceptible to crushing owing to their reduced contact number (Hanley et al. 2015; McDowell and deBono, 2013; Wood and Maeda, 2008).

Effect of Gradation on Void Ratio and Peak Strength: Void ratio indices (e.g. e_{min} , e_{max}) and peak friction angle (φ'_{pk}) as a function of C_U are presented for all mixes in Figures 6a and 6b, respectively. In addition, the final void ratio associated with constant volume conditions at end of shearing (e_{cv}) is also plotted in Figure 6a. The results indicate that void ratio indices (e_{min} , e_{max} , and e_{cv}) decrease, and φ'_{pk} increases, with increasing C_U . The trends show that these quantities converge asymptotically, although not necessarily at the same rates. For example, φ'_{pk} appears to exhibit the greatest sensitivity between a C_U of 1 to 3, whereas void ratio appears to saturate around a C_U of 5.

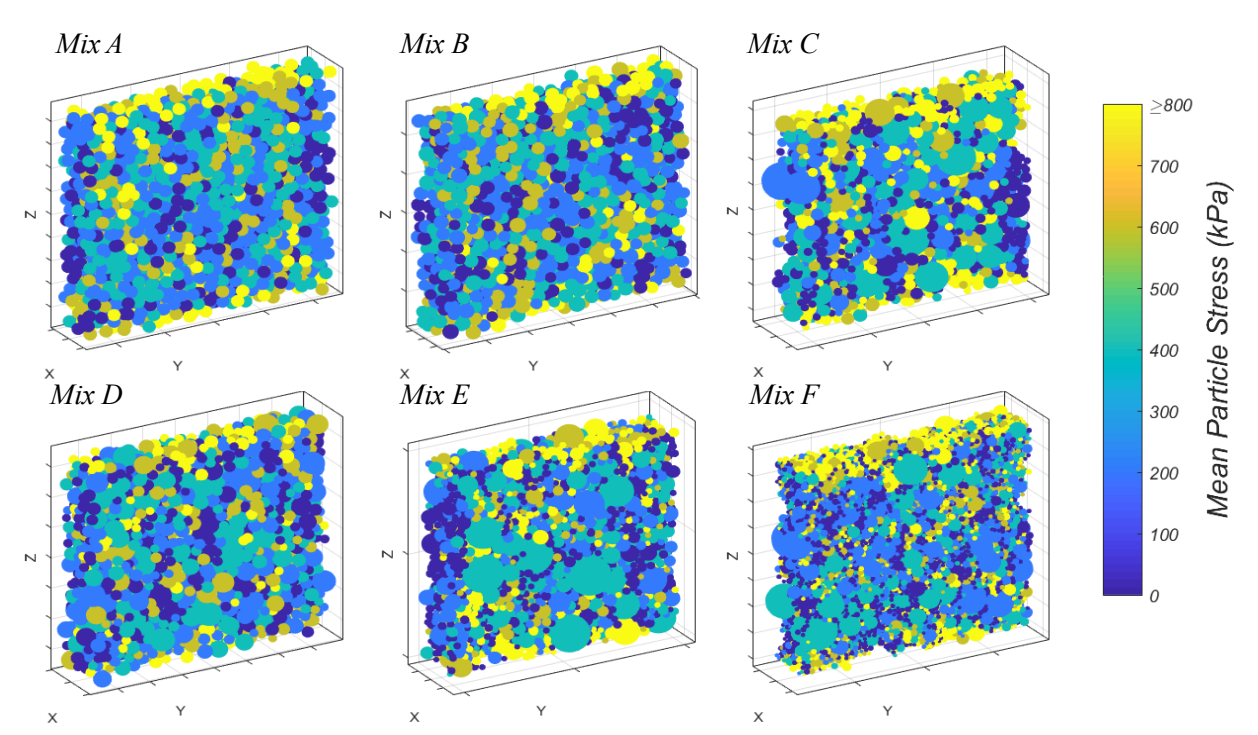


Figure 8. Specimen cross-sections showing mean particle stress at peak stress ratio.

The observed trends of decreasing void indices and asymptotic strength behavior are generally consistent with existing literature from both experimental and numerical studies (e.g. Li et al., 2015; Wood and Maeda, 2008; Youd, 1973). Moreover, the decrease in void indices (e.g. e_{cv}) provides context for understanding how gradation can influence the tendency for soil to contract or dilate when sheared from a critical state perspective (e.g. for the same void ratio, two soils can be loose or dense of critical).

Hypothesized Mechanisms: Figure 7a to 7d shows the coordination number, normalized contact force, contact force, and mean particle stress at the peak response for all mixes. Each of the curves are constructed using averages of histograms associated with a given grain size bin.

Like in Figure 5, floaters and rattlers are omitted when computing averages for bins. A limiting influence of C_U in the quantities is evident as manifested by limiting curves in each space, which appears to mirror the asymptotic behavior seen in mobilized peak strengths of Figure 6b.

Although in this study, C_U is increased from a coarse sand to include coarse gravel (d_{min} to d_{max}), the reverse case from a coarse gravel to include coarse sand (d_{max} to d_{min}) can be regarded analogous. From the latter perspective, the onset of increasing C_U results in an initial increase in stability and strength of the largest particles. However, as particle size distributions become increasingly polydisperse, the effect is a shift towards an infilling-dominated mechanism of the smallest particles. The smallest particles in turn have a diminishing return, or reduced likelihood of contributing significantly to the load-bearing network owing to their low coordination number and contact force magnitudes.

Figure 8 shows vertical sections cut from the center of specimens taken at the peak response with each particle colored-coded by its mean particle stress. For the uniform case (i.e. Mix A), there is a similar likelihood of any particle to carry the lowest stress (as indicated by the darkest colors). However, as the distributions become more widely graded, it is evident that the smallest particles tend to carry the lowest stresses. This is consistent with the previous observations from Figure 5 that the largest particles tend to be clustered around the center of stress distributions.

Bolton's Stress-Dilatancy: The strength of sands is known to depend on their relative density and mean stress at failure (p'f). Bolton's (1986) empirically derived stress-dilatancy relationships represent a commonly used set of correlations for predicting the mobilized strength, or difference of peak and constant volume friction angles $(\varphi'pk - \varphi'cv)$ for sands.

Figure 6c shows ($\varphi'_{pk} - \varphi'_{cv}$) from simulations for $D_R = 100\%$ as a function of C_U . A single φ'_{cv} value computed as the average from all simulations is used on account of numerical and experimental studies which support the observation that gradation has a negligible effect on the constant volume stress ratio (e.g. Yang and Luo, 2017; Jiang et al., 2018). Predictions of ($\varphi'_{pk} - \varphi'_{cv}$) are also calculated directly from D_R and p'_f and shown for comparison in Figure 6c using Bolton's relative dilatancy index and ($\varphi'_{pk} - \varphi'_{cv}$) relationships for triaxial strain with the standard fitting coefficients (Q = 10, R = 1). A very slight decrease in Bolton's predictions is observed due to increasing mean stresses at failure (peak) with increasing C_U , but essentially remains constant.

The results of Figure 6c suggest that Bolton's relationships are perhaps not unreasonable for the present study. However, the correlation clearly does not account for the observed trend of increasing $(\varphi'_{pk} - \varphi'_{cv})$ with gradation. The authors recall that the frictional assignments used in this study are more characteristic of sub-rounded particles, thus the range of $(\varphi'_{pk} - \varphi'_{cv})$ values may be expected to increase using frictional assignments characteristic of even more angular particles.

CONCLUSIONS

The results from a series of numerical simulations of ICD-TXC tests performed with the DEM on specimens of differing particle size distributions (d_{50} of 2.4 to 29.4 mm, C_U of 1.0 to 3.9) with $D_R = 100\%$, and $p'_c = 100$ kPa has led to the following observations and conclusions:

- When particle shape effects are isolated, more widely graded soils can be expected to exhibit greater dilatancy, and higher peak shear strengths for the same D_R .
- How widely graded a granular soil is, rather than absolute size appears to control the mechanical stress-strain response, when ignoring crushing effects.
- Void ratio indices (e_{min}, e_{max}) and the constant volume void ratio (e_{cv}) decreases, and peak

friction angle increases asymptotically with increasing C_U ; the maximum increase in φ'_{pk} is about 4 to 5 degrees using parameters typical of sub-rounded particles, with the greatest sensitivity in C_U appearing to be in the range of 1 to 3.

- Analysis of select fabric quantities reveal several interesting features as a particle size distribution becomes increasingly polydisperse:
 - distributions for contact force, stress, and coordination values also become increasingly disperse;
 - the largest particles most relevant to load bearing tend to sustain the largest contact
 forces and have the highest coordination (resulting in relatively benign stresses) while
 the opposite is observed for the smallest particles.
- It is hypothesized that the asymptotic behavior observed in peak friction angle is attributed to a shift towards an infilling-dominated mechanism, wherein the smallest particles have a reduced probability of contributing in a meaningful way to the load bearing network.
- Stress-dilatancy relationships developed for sands (e.g. Bolton, 1986), may not adequately reflect the range of behaviors expected for widely graded gravels.

Overall, these findings provide an improved understanding of coarse-grained mechanisms which can begin to be used to differentiate a gravelly soil from a sand, as well as defining initial limiting bounds with which to inform future correlation development accounting for particle size effects. Future work intends to extend these findings and implications to an improved understanding of particle size effects on their stress-dilatancy behavior, and cyclic behavior in liquefaction problems.

ACKNOWLEDGEMENTS

Funding for this work is provided by the National Science Foundation (CMMI- 1916152), and the California Department of Water Resources, Division of Safety of Dams. Any opinions, findings and conclusions or recommendations expressed in this material are those of the authors and do not necessarily reflect those of the NSF.

REFERENCES

- Bolton, M.D. (1986). The strength and dilatancy of sands. *Geotechnique*. 36(1), 65-78. Cundall, P. (1988). Computer simulations of dense sphere assemblies. Micromechanics of Granular Materials. 20, 113-123.
- Da Cruz, F., Emam, S., Prochnow, M., Roux, J., Chevoir, F. (2005). Reophysics of dense granular materials: Discrete simulation of plane shear flows. Physical Review, 72, 021309.
- Gonzales, D.B. (2009). Numerical and Experimental Investigation into the Behavior of Granular Materials Under Generalised Stress States. PhD Thesis. University of London, Imperial College.
- Hanley, J.H, O'Sullivan, C., Huang, X. (2015). Particle-scale mechanics of sand crushing in compression and shearing using DEM. *Soils and Foundations*. 55(5),1100-1112
- Hill, R. (1956). The mechanics of quasi-static plastic deformation in metals. In G. Batchelor and R. M. Davies (Eds.), The G.I. Taylor 70th Anniversary Volume, pp. 7–31. Cambridge University Press.
- Huang, X., Hanley, K.J., O'Sullivan, C., Kwok, F.C. (2014). Effect of sample size on the response of DEM samples with a realistic grading. *Particuology*. 15, 107-115.

- Imole O.I., Kumar, N., Magnanimo, V., Luding, S. (2013). Hydrostatic and Shear Behavior of Frictionless Granular Assemblies under Different Deformation Conditions. *Powder and Particle Journal*. 30, 84-108.
- Jiang, M.D., Yang, Z.X., Xie, Y.H. (2018). The influence of particle-size distribution on critical state behavior of spherical and non-spherical particle assemblies. *Granular Matter*, 20(80).
- Li, G., Liu, Y., Dano, C., Hicher, P. (2015). Grading-Dependent Behavior of Granular Materials: From Discrete to Continuous Modeling. *J. Eng. Mech.* 141(6), 04014172.
- Liu, Y., Li, G., Yin, Z., Dano, C., Hicher, P., Xia, X., Wang, J. (2014). Influence of grading on the undrained behavior of granular materials. *Comptes Rendus Mecanique*. 342, 85-95.
- McDowell, G.R., de Bono, J.P. (2013). On the micro mechanics of one-dimensional normal compression. *Geotechnique*. 63(11), 895-908.
- O'Sullivan, C. (2011). Particulate Discrete Element Modelling a Geomechanics Perspective. Spon Press, London.
- Sturm, A.P., Shepard, G.M., DeJong, J.T., Wilson, D.W. (2019). A Centrifuge Study on the Effects of Soil Gradation on CPT Tip Resistance. *Geo-Congress* 2019, Philadelphia, PA.
- Thornton, C. (2000). Numerical simulations of deviatoric shear deformation of granular media. *Geotechnique*. 59(1), 43-53.
- Wood, D.M., Maeda, K. (2008). Changing grading of soil: effect on critical states. *Acta Geotechnica*. 3, 3-14.
- Yi, L.Y, Dong, K.J., Zhou, R.P., Yu, A.B. (2011). Coordination Number of the Packing of Ternary Mixtures of Spheres: DEM Simulations versus Measurements. *Industrial and Engineering Chemistry Research*. 50, 8773-8785.
- Yan, W.M., Dong, J. (2011). Effect of Particle Grading on the Response of an Idealized Granular Assemblage. *International Journal of Geomechanics*. 11(4), 276-285.
- Yang, J., Luo, X.D. (2017). The critical state friction angle of granular materials: does it depend on grading?. *Acta Geotechnica*. 13(3), 535-547.
- Youd, T.L. (1973). Factors Controlling Maximum and Minimum Densities of Sands. *ASTM STP* 523, 98-112.
- Zhang, L., Evans, T.M. (2018). Boundary effects in discrete element method modeling of undrained cyclic triaxial and simple shear element tests. *Granular Matter*. 20(60).